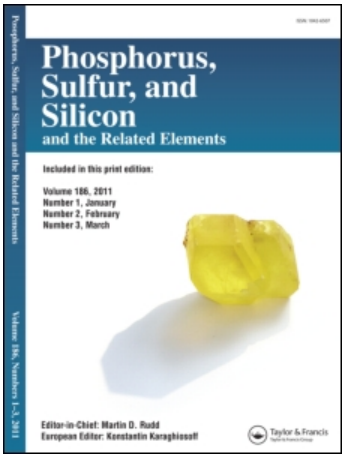

Phosphorus, Sulfur, and Silicon and the Related Elements
Publication details, including instructions for authors and subscription information:
http://www.informaworld.com/smpp/title~content=t713618290

Heterocyclo-Substituted Sulfa Drugs: Part XII. Mercapto-S-Azo-Benzothiazol Dyes and Their Metal Complexes

Ibrahim M. A. Awad[a]; Ahmed H. Osman[a]; Aref A. M. Aly[a]
[a] University of Assiut, Assiut, Egypt

Online publication date: 27 October 2010

To cite this Article Awad, Ibrahim M. A. , Osman, Ahmed H. and Aly, Aref A. M.(2003) 'Heterocyclo-Substituted Sulfa Drugs: Part XII. Mercapto-S-Azo-Benzothiazol Dyes and Their Metal Complexes', Phosphorus, Sulfur, and Silicon and the Related Elements, 178: 6, 1339 — 1352
To link to this Article: DOI: 10.1080/10426500307893
URL: http://dx.doi.org/10.1080/10426500307893

Phosphorus, Sulfur, and Silicon, 178:1339–1352, 2003

ISSN: 1042-6507 print
DOI: 10.1080/10426500390200657

HETEROCYCLO-SUBSTITUTED SULFA DRUGS: PART XII. MERCAPTO-S-AZO-BENZOTHIAZOL DYES AND THEIR METAL COMPLEXES

Ibrahim M. A. Awad, Ahmed H. Osman, and Aref A. M. Aly
University of Assiut, Assiut, Egypt

(Received July 21, 2002; accepted December 10, 2002)

*New azo sulfadrugs of 2-mercapto-S-azo (*p′*-heterocyclo-substituted benzene-sulfonyl) benzothiazole derivatives (L_1 and L_2) were synthesized by coupling of* p′*-heterocyclo-substituted-benzene-sulphonyl diazonium salts with 2-mercapto-benzothiazole in acid medium. The corresponding iron(III), cobalt(II), nickel(II), copper(II), and mercury(II) chelates were prepared in a 1:1 metal to ligand molar ratio. The ligands and their chelates were characterized on the basis of microanalysis, UV, IR, and H^1-NMR spectrometry. Thermal decomposition of the complexes was studied in static air. On the basis of the thermogravimetric curves some decomposition steps could be correlated with the proper decomposition products. The photochemical behavior of the ligands and their complexes were investigated. The photosensitivity shown by the complexes was attributed to the photoreactivity of their free ligands. The ligands and their chelates were screened in vitro for their antimicrobial activities (antibacterial and antifungal). The complexes induce a remarkable increase in the antimicrobial activity compared to the corresponding ligands.*

Keywords: Azo-sulfonamide derivatives; biological screening; mercapto-benzothiazole; metal complexes; photochemical and thermal studies

Sulfonamide and azo-sulfonamide derivatives have been found to be biologically versatile anticancer,[1] antimalarial,[2] and antitubercular[3] drugs. It also has been reported that the replacement of the carbonyl oxygen by a sulfur in some heterocyclic compounds enhances the fungicidal activity.[5,6] In view of biological importance of these compounds, and in continuation[7–9] of our interest in azo-sulfonamide derivatives,[10–12] we report on the preparation of some new azo sulfa drugs based on 2-mercapto-benzothiazole containing two

Address correspondence to I. M. Awad, Department of Chemistry, Faculty of Science, Assiut University, Assiut 71516, Egypt. E-mail: ibrahimawad@yahoo.com

heterocyclic-substituted moieties in the *p*-position of the sulfonamide part, namely: 4′-(2″-pyrimidylaminosulfonyl) aniline (L_1) and/or 4′(2″-(dimethyl) pyrimidylaminosulfonyl)aniline (L_2), and their chelates Fe(III), Co(II), Ni(II), Cu(II), and Hg(II) to improve the pharmacological properties of the mercaptobenzothiazoly-azo sulfornamide derivatives.

EXPERIMENTAL

All the reagents and solvents required for the preparation of the compounds were of AR grade.

p-*[(p′-Heterocyclo-substituted)sulfonyl]benzene Diazonium Chlorides*

These compounds were prepared by diazotization of *p*′-amino benzene- sulphonyl derivatives (sulfa diazine and/or sulfa dimidine) (0.01 mmol) in a mixture of either ethanol or acetone and 40 ml of 70% pure hydrochloric acid with sodium nitrite (0.01 mmol) at 0–5°C. The diazonium salts were allowed to react immediately without separation for the synthesis of the corresponding azo dye sulfa drug compounds.

Synthesis of 2-Mercapto-S-azo[(p′-heterocyclo-substituted Benzenesulfonyl)]benzothiazole Derivatives (L_1 and L_2)

To a solution of 2-mercapto-benzothiazole (0.05 mmol) in 50 ml of 15% sodium hydroxide, an appropriate diazonium salt of the free *p*′-aminobenzene sulphonamide derivatives (0.01 mmol) was added portionwise with stirring. The temperature was maintained at 5–10°C, and stirring was continued for 2 h. The reaction mixture was accompanied by a change in color from pale to deep yellowish red, and was kept at the ambient temperature for 4 h more. When the product was precipitated, an excess of cold water was then added and the product was filtered, washed well with water, dried, and recrystallized from ethanol. The physical and chemical data of azo-mercaptobenzothiazole derivatives (L_1, L_2) are quoted in Table I.

Preparation of Fe(III), Co(II), Ni(II), Cu(II), and Hg(II) Azo-Mercaptobenzothiazole Chelates

The hot ethanolic solution of the ligand (0.02 mmol) was added dropwise under stirring to a solution of the respective metal chloride (0.02 mmol) in ethanol (20 ml); stirring at 70–80°C was continued for 40 min. The reaction mixture was cooled and the precipitated product was filtered, washed thoroughly with distilled water, dried, and recrystallized from ethanol (Table I).

TABLE I Physical and Analytical Data of the Ligands and Their Complexes

Compound	m.p.°C (decmp.)	Yield %	Microanalysis %C(calc.)	%H(calc.)	%N(calc.)	%S(calc.)
L_1	157	92	46.56 (47.62)	2.91 (2.82)	20.83 (19.62)	21.97 (22.45)
L_2	183	91	50.10 (49.96)	3.82 (3.53)	1962 (18.41)	22.01 (21.08)
$[Fe(L_2)Cl_3](H_2O)] \cdot 3H_2O$	255	82	32.13 (33.04)	3.03 (3.47)	11.80 (12.17)	14.21 (13.92)
$[Co(L_1)Cl_2] \cdot 2H_2O$	238	73	33.52 (33.35)	2.43 (2.71)	13.85 (14.14)	15.26 (16.18)
$[Co(L_2)Cl_2] \cdot 2H_2O$	249	76	35.01 (36.67)	3.50 (3.23)	14.11 (13.49)	15.93 (15.45)
$[Ni(L_2)Cl_2(H_2O)_2]$	258	73	37.53 (38.93)	2.91 (2.75)	14.25 (14.36)	15.97 (16.41)
$[Cu(L_1)Cl_2] \cdot 2H_2O$	218	85	35.59 (36.07)	2.68 (2.86)	15.55 (14.93)	16.59 (17.08)
$[Hg(L_1)Cl_2] \cdot 2H_2O$	201	70	26.81 (27.74)	3.02 (2.19)	12.17 (11.42)	12.35 (13.08)

L_1:

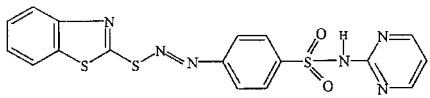

L_2:

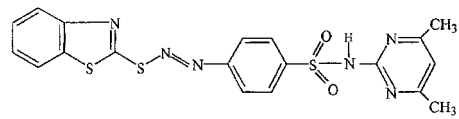

Physical Measurements

All melting points were determined on a melting point apparatus and were uncorrected. H-^{1}NMR were recorded on a Varian EM-390 MHz spectrometer in deuterated d_6DMSO as a solvent using TMS as internal standard. Elemental analyses were performed on a Perkin-Elmer 240 E microanalyser. The infrared spectra were recorded as KBr pellets on a 470 Shimadzu infrared spectrophotometer. The electronic spectra were carried out in DMF solution on a UV-2101 PC Shimadzu spectrophotometer.

The thermogravimetric analyses were determined in a static air using an electrobalance of the type Sartorius 200 MP converted to a thermobalance by addition of a small furnace and sample holder. The temperature was measured using a Chromal-Alumal thermocouple attached to a digital multimeter type Soar ME 550; the heating rate was adjusted to 8°C min^{-1}.

Photolyses were achieved using an Osram HBO 200 w/2 lamp as light source. Monochromatic light was obtained using the Schott IL interference filter 336 nm. Irradiation was carried out in solutions of DMF in 1-cm spectrophotometer cell at room temperature. Progress of the photolyses was monitored by the above mentioned spectrophotometer.

BIOLOGICAL ACTIVITY

Antibacterial and Antifungal Screening

The disc-diffusion method[16,17] was used to measure the antibacterial activity. The antibacterial activity of the ligands and their chelates

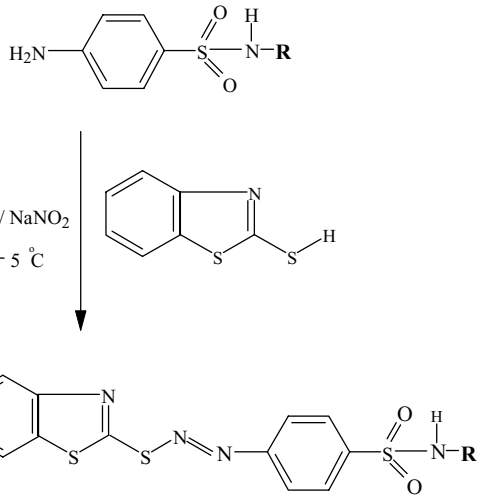

Ligand No.	R
L_1	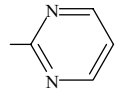
L_2	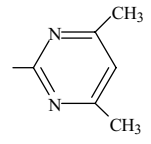

SCHEME 1

was tested with three strains of bacteria namely: *Staphylococcus aureus, Bacillus cereus*, and *Micrococcus roseus*. The antifungal effect was tested with three species of fungi namely: *Aspergillus flavus, Aspergillus niger*, and *Penicllium chrysogenum*.

RESULTS AND DISCUSSION

The azo dyes of S-azo(*p*-heterocyclo-substituted benzene-sulfonamido-)-2-mercapto-benzothiazole were synthesized by diazotization of *p*-aminobenzene-*p*′-substituted heterocyclo sulphon-amides at 0–2°C in acetic acid and hydrochloric acid (1:4 molar ratio) solution and coupling with 1.5 mmol of 2-mercaptobenzothiazole in sodium hydroxide solution to give the corresponding azo dye ligands at pH 6.5 (Scheme 1). The corresponding iron(III), cobalt(II), nickel(II), copper(II), and mercury(II) chelates were prepared in a 1:1 molar ratio of metal:ligand by the interaction of an ethanolic solution of the ligand with an ethanolic solution of the metal salt.

The ^{1}H-NMR spectra of L_1 and/or L_2 were recorded on a EM-390 MHz spectrophotometer using d_6-DMSO as solvent with TMS as the internal standard. The ^{1}H-NMR spectra are in good accordance with the following signals: at $\delta = 7.75$–6.65 ppm (m, 9 H and/or 11 H, aromatic protons), at δ 2.25 ppm (S, 3H, CH_3 groups) for L_2 and at δ 9.90 ppm (S, 1 H, SO_2.NH) which removed by using D_2O treatment.

Infrared Spectra

The IR spectra of the ligands and their complexes (Table II) show two bands at 1310–1325 cm^{-1} and 1140–1160 cm^{-1} for ν_{asy}. S=O and ν_{sy}. S=O respectively. The absence of large systematic shifts of the $-SO_2$ stretching frequencies in the spectra of the complexes compared to those of the ligands implies that there is no interaction between the sulphonyl groups and the metal ions.

As would be expected, the characteristic vibrational mode of the −N=N− group occurs at 1450–1462 cm^{-1}. This absorption frequency range is essentially the same for the free ligands and their complexes. Even though direct evidence for bonding via the azo group is lacking, the molecular models show that the azo group should be one of the coordination sites in the ligands. ν C=N, which appears in the free ligands as a band at 1590–1595 cm^{-1}, splits in the case of $[Fe(L_2)Cl_3(H_2O)] \cdot 3H_2O$, $[Co(L_2)Cl_2(H_2O)_2]$, and $[Cu(L_1)Cl_2] \cdot 2H_2O$ into two components lying between 1570–1620 cm^{-1}. This splitting is believed to be an indication of coordination of the ligand through the nitrogen atom of the heterocyclic ring.

TABLE II Infrared and Electronic Spectral Bands of the Ligands and Their Complexes

Compound	IR spectra (cm^{-1})					
	νN=N	$\nu_{asy.}$ SO_2	$\nu_{sy.}$ SO_2	νNH+ νOH(H_2O)	νC=N	Electronic spectra (nm)
L_1	1456	1310	1158	3450	1590	277, 273
L_2	1455	1310	1140	3400	1595	277, 273
$[Fe(L_2)Cl_3(H_2O)] \cdot 3H_2O$	1461	1310	1160	3350	1590 1620	334, 273
$[Co(L_1)Cl_2] \cdot 2H_2O$	1462	1310	1160	3450	1580	277, 273
$[Co(L_2)Cl_2] \cdot 2H_2O$	1462	1310	1160	3450	1570 1580	327, 295, 277
$[Ni(L_2)Cl_2(H_2O)_2]$	1460	1310	1150	3400	1580 1580	590, 407, 329, 289, 273
$[Cu(L_1)Cl_2] \cdot 2H_2O$	1450	1310	1150	3450	1590 1620	413, 277, 273
$[Hg(L_1)Cl_2] \cdot 2H_2O$	1440	1325	1158	3450	1580	277, 273

Electronic Spectra

The electronic spectra of the ligands and their complexes are recorded in DMF. The spectral bands are tabulated in Table II. The spectra of the ligands are characterized by an intense band at 273 nm attributed to a $\pi \rightarrow \pi^*$ transition. This band is associated with a well defined shoulder at 277 nm, which we assign to a transition of the type $n-\pi^*$.

The complexes of L_1, namely those of Co(II), Ni(II), and Hg(II) exhibit more or less the same spectral pattern as the ligand; the Cu(II) complex, however, displays in addition a band at 413 nm, probably associated with a charge transfer transition.

For the complexes of L_2, the spectrum of Fe(III) exhibits two bands at 334 nm and 273 nm, which are ascribed to charge transfer and intraligand transitions respectively. The Co(II) complex shows an intense band at 329 nm assignable to a charge transfer transition. The band at 273 nm and its associated shoulder at 295 nm are interaligand transitions. The Ni(II) complex shows a d–d band at 590 nm, which can be related to the transition $^3T_{1g} \leftarrow {}^3A_{2g}$ typical of six coordinate Ni(II) complexes. The complex exhibits further two bands at 409 nm and 329 nm, which in view of its intensity and position, are assigned to charge transfer transitions. This complex displays also two bands at 289 nm and 273 nm due to intraligand transitions.

Thermal Decomposition

The thermal decomposition of the complexes was studied in a static air in the range from ambient temperature to 500°C.

The iron complex $[Fe(L_2)Cl_3(H_2O)]\cdot 3H_2O$ undergoes a stepwise decomposition in three stages well discernible in the TG and DTG curves. The first step (between 120 and 200°C) is commensurate with the release of four water molecules (calc. 10.4% found 11.0%). This step is accompanied by an activation energy of 17.1 KJ mole^{-1}; the small value of activation energy indicates a rather fast dehydration of crystal water molecules which are loosely bonded. The coordinated water molecule seems to be attached via ion–dipole interaction to the Fe(III) and consequently was lost together with the three crystal water molecules[11]. The second and third steps correspond to the decomposition of the anhydrous complex. The second step (260–360°C) correlates well with the loss of $N_2 + 3Cl+$ organic radical (I) (calc. 43.3% found 43.8%). The organic radical may dimerise to compound (**II**) or abstract H· to form compound (**III**) (Eq. 1 and 2) before it decomposes. The third step occurs in the temperature range 380–480°C and relates to the decomposition of the rest of the organic ligand. The end product is Fe_2O_3 (calc. 22.9%, found 22.0%).

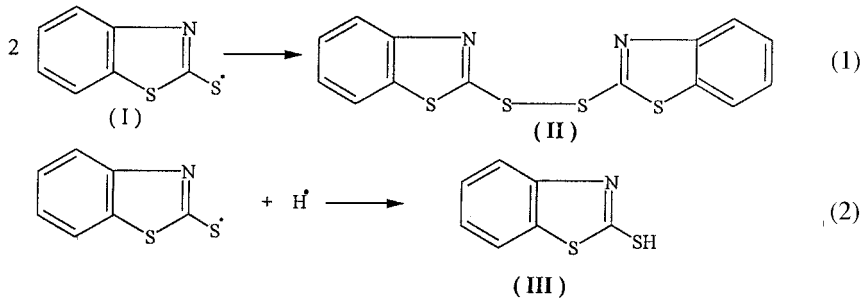

The thermolysis curve of the cobalt complex, $[Co(L_2)Cl_2]\cdot 2H_2O$ indicates two decomposition steps in the range 80–155 and 280–400°C. The mass loss at the first step points to the elimination of two water molecules with an activation energy of 19.2 KJ/mole, in the range expected for lattice water.[12] The anhydrous complex decomposes then in one step, namely the second step with a weight loss of 69.1%. At ~400°C the residual mass (24.1%) is greater than the calculated for $CoCO_3$ (20.3%). It is possible that part of the carbon liberated from the thermal decomposition of the ligand is included in the residue. The activation energy for this step amounts to 132.4 kJ mol^{-1}.

For the complex $[Ni(L_2)Cl_2(H_2O)_2]$, the stepwise course of the theromogravimetric curve is characterised by two steps in the temperature ranges 60–140 and 200–280°C (Figure 1). The first step seems to include the loss of the two coordinated water molecules together with other decomposition products (30.0%) and the observed weight loss at the second step is 45.0%. Unfortunately it was difficult to

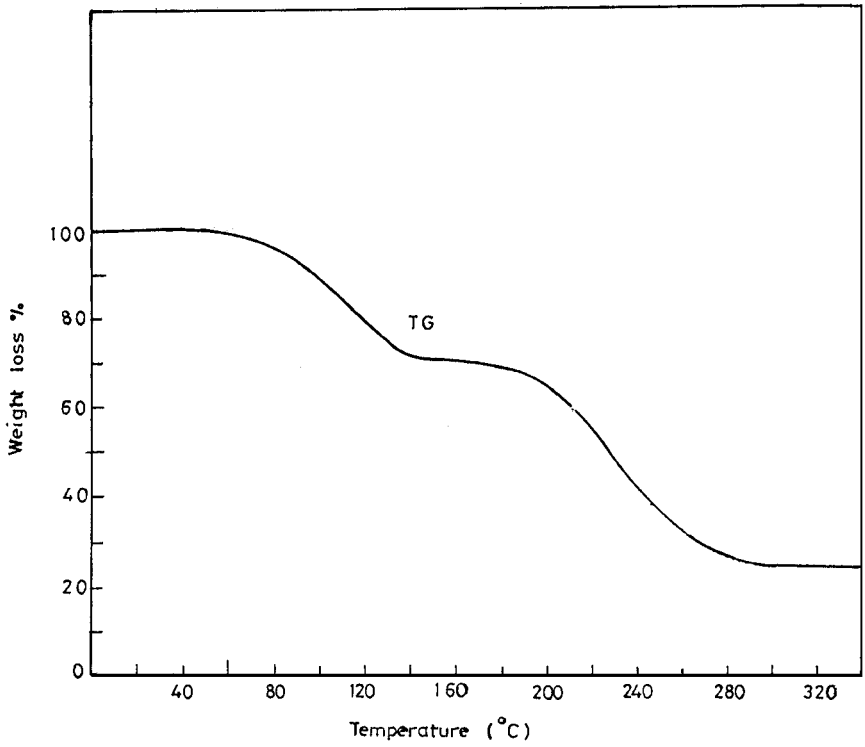

FIGURE 1 TG thermogram of $[Ni(L_2)Cl_2(H_2O)_2]$.

correlate the first and second steps with the proper decomposition products.

For the complex $[Cu(L_1)Cl_2)] \cdot 2H_2O$, two separate successive steps are observed. The first step (calc. 51.3% found 51.9%) accounts for the loss of:

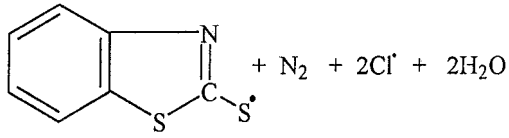

The organic radical may react with a hydrogen radical or dimerize before it decomposes. The remaining organic moiety decemposes in the second step. The overall loss of mass from the TG curve is 79.0% leaving $CuCO_3$ as the final residue (21.0%).

The TG profile of $[Hg(L_1)Cl_2] \cdot 2H_2O$ exhibits two decomposition steps in the temperature range 50–80 and 260–380°C. The first stage is consistent with the expulsion of two water molecules (calc. 4.9%, found 5.3%). The low temperature range indicates that the water molecules

are weakly bonded in the lattice. The second step is a major step (85.2%) and corresponds to the decomposition of almost all the organic moiety. This step has an activation energy of 47.6 kJ/mmol. The residue, which amounts to 9.9% is much less than calculated for HgO (29.9%), indicating extensive decomposition of the mercuric oxide.

For evaluating the kinetic parameters, the Coats–Redfen equation[13] was used. For $n \neq 1$ and $n = 1$ (n = order of the reaction) the following two equation are indicated:

$$\ln\left[\frac{1-(1-\alpha)^{1-n}}{(1-n)T^2}\right] = M/T + B \quad \text{for } n \neq 1 \tag{3}$$

$$\ln\left[\frac{-\ln(1-\alpha)}{T^2}\right] = M/T + B \quad \text{for } n = 1 \tag{4}$$

where $M = -E/R$ and $B = \ln ZR/\phi E$;

E, R, Z, and ϕ are the activation energy, gas constant, pre-exponential factor, and heating rate respectively. The correlation coefficient (***r.***) is computed using the least squares method for Eq. 3 and 4. Linear curves were drown for (n) values ranging from 0 to 2. The value of (n) which gave the best fit was chosen as the order parameter for the decomposition stage of interest. The kinetic parameters were calculated from the plots of left hand side of Eq. 3 and 4 against 1/T. The kinetic parameters (n and E) are calculated according to the above two equations and cited in Table III.

TABLE III Kinetic Data of the Complexes

Compound/Step	E kJ/mol	n	*r*
$[Fe(L_2)Cl_3(H_2O)] \cdot 3H_2O$			
Step I	17.1	1	0.9777
Step II	78.9	2	0.9979
$[Co(L_2)Cl_2] \cdot 2H_2O$			
Step I	19.2	1	0.9987
Step II	132.4	2	
$[Ni(L_2)Cl_2(H_2O)_2]$			
Step I	50.0	1	0.9993
Step II	107.4	2	0.9935
$[Cu(L_1)Cl_2] \cdot 2H_2O$			
Step I	149.7	2	0.9885
Step II	71.1	0.66	
$[Hg(L_1)Cl_2] \cdot 2H_2O$			
Step II	47.6	0.66	0.9592

E = activation energy.
n = order of the decomposition reaction.

In conclusion, the thermal decomposition of the complexes occurs in a stepwise manner. The activation energies of the decomposition steps are low, which indicates the relative low stabilities of the present complexes.

Photochemical Studies

Solutions of the complexes under investigation in DMF are light sensitive. The photolysis is accompanied by spectral changes commensurate with photodecomposition of the complexes. All studied complexes exhibit the same behavior; so the spectral changes associated with photolysis of $[Ni(L_2)Cl_2(H_2O)_2]$ is taken as representative (Figure 2). Upon irradiation of the Ni-complex solution at 336 nm, a decrease in the absorption at ~329 nm was noticed. It seems that the active excited state reached by light absorption is of the internal ligand excited state type (IL). The following reaction is postulated to account for our results:

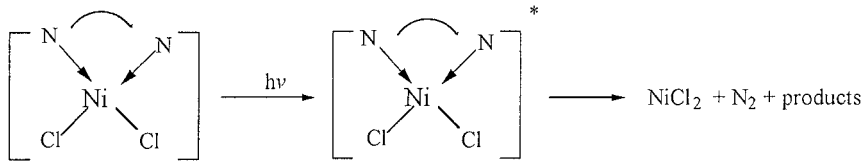

IL - excited state

where $\overset{\frown}{N\quad N}$ represents the ligand.

The spectral changes observed during irradiation of DMF solution of the free ligand (L_2) show a decrease in the absorption at ~277 nm. (Figure 3). This indicates that the ligand decomposes giving N_2- molecules. It is well known that compounds containing nitrogen—nitrogen double bonds exhibit extreme photoreactivity due to the stability of the photoelimination product, dinitrogen.[14] A related interpretation has been applied to the photolysis of mixed ligand complexes of Cu(II) containing 5-arylazo-8-hydroxyquinoline derivatives and alkyl xanthates.[15] In conclusion it is shown that the photoreactivity of the studied complexes is mainly due to the photosensitivity of the ligand.

BIOLOGICAL EVALUATION

Antibacterial Activity

The antibacterial results revealed that the ligands and their metal Fe(III), Co(II), Ni(II), Cu(II), Hg(II) chelates exhibit pronounced

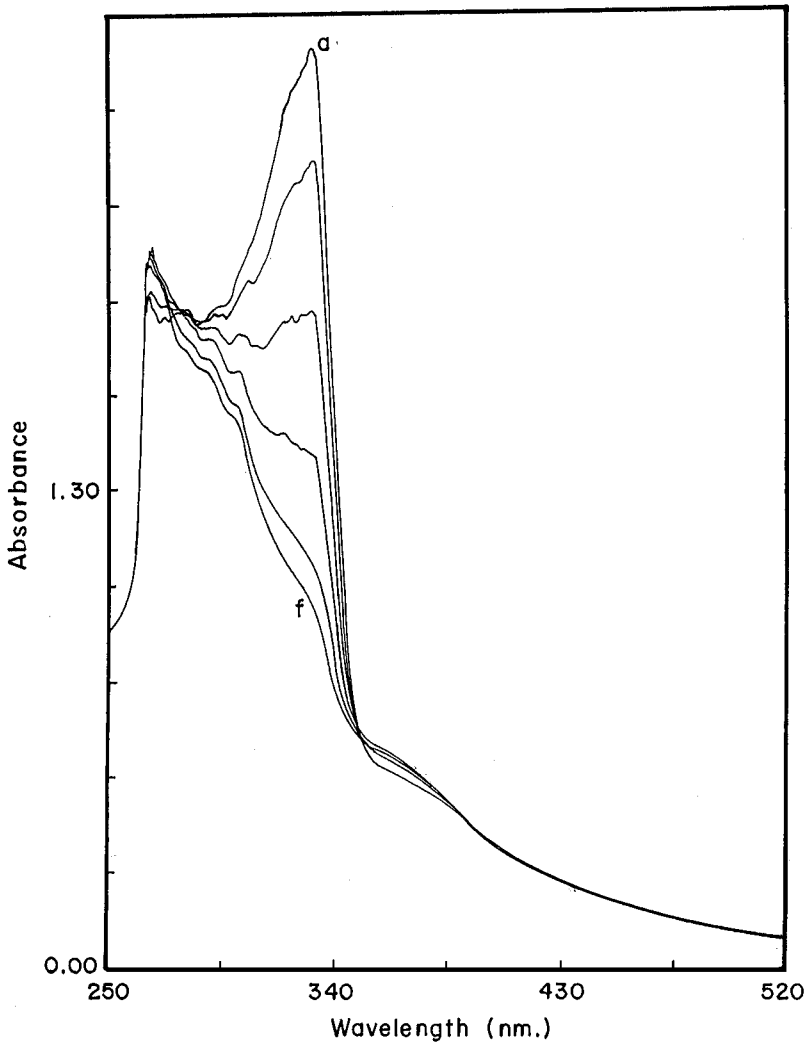

FIGURE 2 Spectral changes during photolysis of $[Ni(L_2)Cl_2(H_2O)_2]$ solution in DMF at 0(a), 10, 20, 30, 40, and 60(f) min irradiation time, $\lambda_{irr} = 336$ nm; 1 cm cell.

activities against all of the test bacteria (inhibition zones ranged from 7.0–35.0 mm). Mercury chelate is very active (inhibition zones 7.0–22.0 mm) more than iron copper and cobalt chelates (c.f. Table IV). Furthermore, nickel chelate represents the most effective compound than the others metal chelates, (inhibition zones 16–40 mm) against

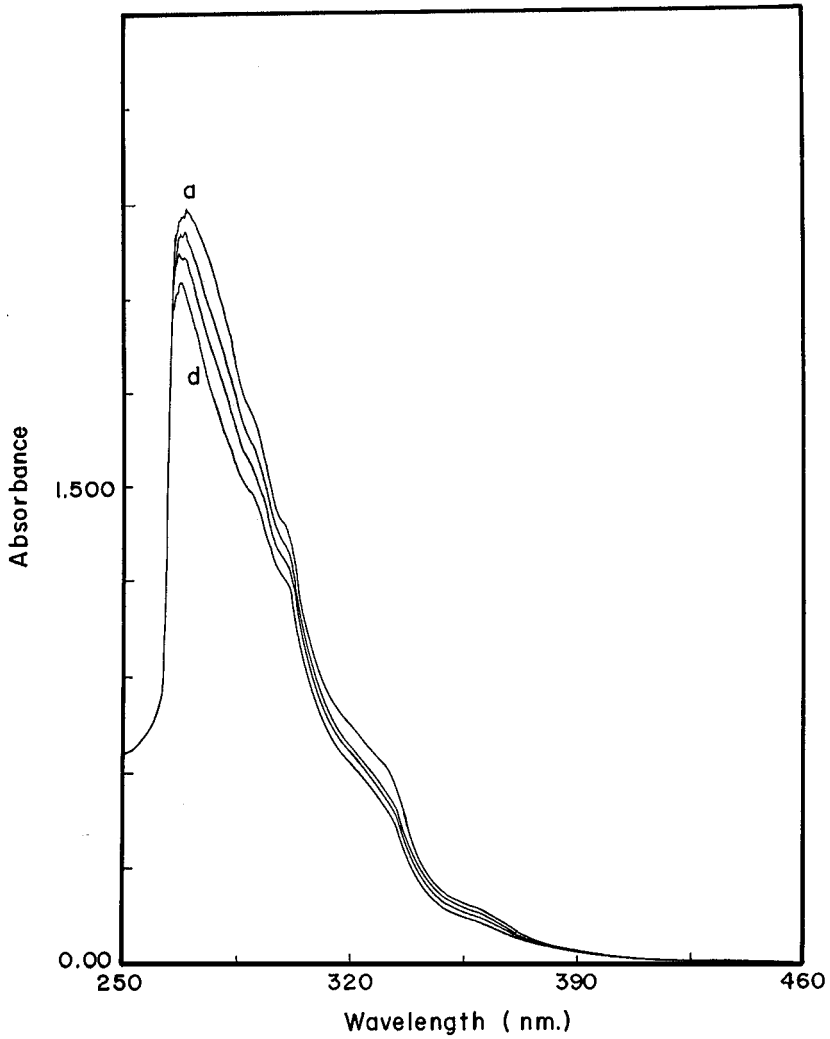

FIGURE 3 Spectral changes during the photolysis of (L_2) solution in DMF at 0(a), 20, 50, and 60(d) min irradiation time, $\lambda_{irr} = 336$ nm; 1 cm cell.

the used bacteria.[16,17] The mercapto-bezothiazolo sulfa drugs (ligands) are comparatively more active against the test bacteria than the free *p*-aminobezo-sulphonamide derivatives.

From the antifungal activities, it was found that some of the ligands and their chelates showed variable activities (inhibition zones 7.0–40.0 mm) against the fungi used. The mercury chelate is more active (20.0–30.0 mm) than iron, copper, and cobalt chelates. Interestingly,

TABLE IV Antimicrobial Activity of Ligands (L_1 and L_2) and Their Metal Chelates (Inhibition Zones in mm)

	Antibacterial activity			Antifungal activity		
Compound no.	*Staphylococcus aureus*	*Bacillus cereus*	*Micrococcus roseus*	*Aspergillus flavus*	*Aspergillus niger*	*Penicllium chrysogenum*
L_1	6.00 (−ve)	4.00 (−ve)	9.00 (−ve)	9.00 (5.00)	8.00 (6.00)	12.00 (−ve)
$[Co(L_1)Cl_2] \cdot 2H_2O$	12.00	6.00	10.00	20.00	25.00	24.00
$[Cu(L_1)Cl_2] \cdot 2H_2O$	7.00	8.00	13.00	(−ve)	10.00	7.00
$[Hg(L_1)Cl_2] \cdot 2H_2O$	5.00	5.00	6.00	(−ve)	7.00	12.00
L_2	8.00 (−ve)	12.00 (−ve)	9.00 (−ve)	−ve (−ve)	8.00 (6.00)	12.00 (8.00)
$[Fe(L_2)Cl_3 \cdot (H_2O)] \cdot 3H_2O$	1.00	−ve	−ve	−ve	9.00	−ve
$[Co(L_2)Cl_2] \cdot 2H_2O$	12.00	14.00	11.00	7.00	−ve	7.00
$[Ni(L_2)Cl_2 \cdot (H_2O)_2]$	20.00	17.00	21.00	12.00	19.00	20.00

(−ve) = biological inactive.

all nickel chelates are highly active against all fungi used compared to other metal chelates (inhibition zones ranged from 25.0–40 mm). All newly synthesized compounds show more fungicidal than bactericidal effects.[16,17]

REFERENCES

[1] H. La Roche and A. G. Co, Swiss Patent, Neth. Apt. 66610, 566 (Cl. CO 7d). 31; *Chem. Abstr.*, **67,** 733 23r (1967).
[2] L. H. Schimdt, *Ann. Rev. Microbiol.*, **23,** 427 (1977).
[3] A. J. Vaichulis, U.S. Pat. 8273352 (1977).
[4] S. Moeschlin and U. S. Schnider, *New Eng. J. Med.*, **57,** 369 (1963).
[5] S. Rao and S. A. Mittra, *Indian J. Chem.*, **15B,** 1062 (1977).
[6] K. S. Mohanty, R. Sridhar, Y. S. Padwanava, R. Sounder, and A. S. Mittra, *Indian J., Chem.*, **15B,** 1146 (1977).
[7] A. A. Abdel Hafez, I. M. A. Awas, and Kh. M. Hassan, *Coll. Czech. Chem. Commun.*, **52,** 2753 (1987).
[8] I. M. A. Awad, A. M. A. Aly, A. M. Abdel-Alim, R. A. Abdel-Aal, and S. H. Ahmed, *J. Inorganic Biochemistry*, **33,** 77 (1988).
[9] I. M. A. Awad and A. M. A. Aly, *J. Synth. React, Inorg. Met-Org. Chem.*, **21,** 375 (1991).
[10] I. M. A. Awad, *Phosphorus, Sulfur, and Silicon*, **114,** 17 (1996).
[11] H. Icbudak, V. T. Yilmaz, and H. Olmez, *J. Therm. Anal.*, **53,** 843 (1998).
[12] J. Garcia, M. C. Molla, J. Borras, and E. Escriva, *Thermochim. Acta*, **106,** 155 (1986).
[13] A. W. Coats and J. P. Redfern, *Nature*, **20,** 68 (1946).
[14] H. Rau Angew, *Chem. Internat. Edit Eng.*, **12,** 224 (1973).
[15] A. H. Osman, A. S. A. Zidan, A. I. El-Said, and A. A. M. Aly, *Transition Met. Chem.*, **18,** 34 (1993).
[16] K. K. Chaturred, Jain Nok, P. Jain, and R. Kaushal, *Indian Drug*, **15,** 57 (1978).
[17] J. D. Sleight and M. C. Timburg, Notes on Medical Bacterology (Churchill Livingston, C. S. A., 1981), p. 43.